

Helicobacter pylori regulates iNOS promoter by histone modifications in human gastric epithelial cells

Tiziana Angrisano · Francesca Lembo ·
Silvia Peluso · Simona Keller · Lorenzo Chiariotti ·
Raffaella Pero

Received: 23 September 2011 / Published online: 5 January 2012
© Springer-Verlag 2012

Abstract Inducible nitric oxide synthase (iNOS) expression is altered in gastrointestinal diseases. *Helicobacter pylori* (*Hp*) infection may have a critical role in iNOS dysregulation. We undertook this study to investigate possible chromatin changes occurring early during iNOS gene activation as a direct consequence of *Hp*–gastric cells interaction. We show that *Hp* infection is followed by different expression and chromatin modifications in gastric cells including (1) activation of iNOS gene expression, (2) chromatin changes at iNOS promoter including decreased H3K9 methylation and increased H3 acetylation and H3K4 methylation levels, (3) selective release of methyl-CpG-binding protein 2 from the iNOS promoter. Moreover, we show that *Hp*-induced activation of iNOS is delayed, but not eliminated, by the treatment with LSD1 inhibitors. Our data suggest a role for specific chromatin-based mechanisms in the control of human iNOS gene expression upon *Hp* exposure.

Tiziana Angrisano and Francesca Lembo contributed equally to this work.

Electronic supplementary material The online version of this article (doi:10.1007/s00430-011-0227-9) contains supplementary material, which is available to authorized users.

T. Angrisano · S. Peluso · S. Keller · L. Chiariotti (✉) ·
R. Pero (✉)

Dipartimento di Biologia e Patologia Cellulare e Molecolare
“L. Califano”, Facoltà di Scienze Biotechnologiche and Facoltà
di Farmacia, Università degli Studi di Napoli “Federico II”,
via S. Pansini 5, 80131 Naples, Italy
e-mail: pero@unina.it

F. Lembo · S. Keller · L. Chiariotti
Dipartimento di Chimica Farmaceutica e Tossicologica, Facoltà
di Farmacia, Università degli Studi di Napoli “Federico II”,
Naples, Italy

Keywords *Helicobacter pylori* ·
Chromatin modifications · iNOS · Gastric cells

Introduction

Helicobacter pylori (*Hp*) is a Gram-negative bacterium involved in several gastric diseases. Persistent infection with *Hp* may cause in humans chronic atrophic gastritis, with development of intestinal metaplasia, dysplasia and gastric carcinoma [1–6] as also demonstrated in animal models [6–8]. Therefore, *Hp* is classified as a carcinogenic agent class I. The mechanism of *Hp* pathogenicity is not well understood, although both bacterial virulence and host susceptibility factors have been associated with the development of chronic gastric inflammation and gastric carcinogenesis [6–11].

Hp, through TLRs receptors, induces expression of host inflammatory genes such as TNF- α , which in turn activates NF- κ B, a transcription factor whose target genes include iNOS [12–15]. Recent advances in basic research on *Hp*-associated carcinogenesis have gradually clarified that nitric oxide (NO)-derived iNOS plays a crucial role in the process of gastric carcinogenesis [16, 17]. It has been reported that iNOS is expressed in gastric mucosa from patients with *Hp*-induced gastritis and that this expression is closely related to inflammatory cell infiltration in the gastric mucosa [18]. A great deal of evidence supports a role of iNOS in promoting tumour development. A number of activities may contribute to the tumour-enhancing effects of NO, including DNA damage [19], increased angiogenesis and blood flow [20], prevention of apoptotic cell death [21], activation of iNOS [22] and suppression of the immune system [23]. Therefore, chemoprevention by antioxidants or treatment against *Hp* was proposed

and showed reducing the incidence of gastric cancer [16, 24].

It has been suggested that epigenetic controls on iNOS transcription may be operative. Specific studies on iNOS have shown that lower DNA methylation in the gene promoter is associated with increased expression and that the human iNOS promoter was basally enriched with methylation of H3 lysine 9 in endothelial cells [25]. Although much is known about the *cis*- and *trans*-regulatory factors controlling activation of iNOS transcription by cytokines and bacterial lipopolysaccharide (LPS), relatively little is known about how local changes in chromatin structure might participate in this process. A critical and still unanswered question is whether epigenetic changes observed in gastric diseases may be a direct consequence of *Hp* infection. To date, a few studies have addressed the possibility that *Hp*-induced host target genes activation may be controlled by epigenetic mechanisms. One recent study indicated that a change in H3S10 phosphorylation status at IL-6 gene promoter is related to *Hp* infection through NF- κ B/ERK/p38 pathway [26]. We have recently demonstrated that chromatin and DNA methylation modifications accompany *Hp*-induced Cox-2 activation in gastric epithelial cells [27] and LPS-induced IL-8 activation in human intestinal epithelial cells [28]. In this work, we hypothesized that *Hp* infection may have a direct impact on epigenetic status of iNOS gene in gastric cells and that the *Hp*-induced iNOS activation may be mediated by histone modifications at iNOS gene regulatory regions. Our data suggest a role for specific chromatin-based mechanisms in the control of human iNOS gene expression upon *Hp* exposure.

Materials and methods

Human gastric epithelial cell culture

MKN 28 cell line was derived from a human gastric tubular adenocarcinoma and shows moderate gastric-type differentiation; this cell line has proven to be a suitable in vitro model for the study of interactions between *Hp* and the gastric epithelium [29, 30]. MKN 28 cells were grown as monolayers in DMEM Ham's nutrient mixture F-12 (1:1; Sigma, St. Louis, MO) supplemented with 10% FCS (Life Technologies, Inc.) at 37°C in a humidified atmosphere of 5% CO₂. Tranilcyproline (TCP) and pargyline were from Sigma.

Bacterial strains and coculture conditions

Hp strains used in this study were *Hp* wild-type strains 60190 (ATCC 49503, VacA+/cag PAI+) and CCUG

17874 (National Collection of Type Cultures, London, England, 11637, VacA+/cagPAI+) containing the *cag* pathogenicity island and secreting an active form of VacA [31]. In contrast, the *Hp* mutant strain Tx30a (ATCC 51932, VacA-/cag PAI-) [32] lacks the *cag* pathogenicity island and is unable to translocate CagA product into the host gastric epithelial cells and produces a VacA protein that fails to induce vacuolation in vitro [33, 34]. In addition, we also used *E. coli* strain DH5 α (Stratagene). Bacteria were grown in brucella broth (DIFCO Laboratories, Detroit, MI) supplemented with 1% Vitox (Oxoid, Basingstoke, UK) and 5% FCS (Life Technologies, Inc., Paisley, UK) for 24–36 h at 37°C in a thermostatic shaker under microaerobic conditions. Bacteria were harvested by centrifugation and added to gastric cells at concentration of 5×10^7 CFU/ml in DMEM supplemented with 10% FCS at a multiplicity of infection (MOI) of 100. Cells were incubated in the absence (controls) or in the presence of bacteria for the indicated times. As controls, we also used the CCUG 1784 (VacA+/cag PAI+) *Hp* strain, the VacA-/cag PAI- *Hp* strain Tx30a and the *E. coli* strain DH5 α (Stratagene). The cells were suspended in phosphate-buffered saline (PBS), and the density was estimated by spectrophotometry (A405) and by microscopic observation. To avoid the influence of serum, gastric cells were starved for 16 h before and throughout the period of treatment in all experiments.

Preparation of cell extracts and Western blot analysis

After incubation with *Hp*, cells were rapidly washed twice with PBS to remove bacteria, then lysed in RIPA buffer (PBS containing 1% Nonidet P 40, 0.5% sodium deoxycholate, 0.1% SDS, 100 ng/ml phenylmethyl sulfonyl fluoride and 10 μ g/ml aprotinin). The samples, containing 50 μ g protein per lane, were resolved by electrophoresis using 12% SDS-PAGE precast gels (Bio-Rad Laboratories, Milan, Italy) as appropriate and transferred to BA 85 0.45 m PROTAN nitrocellulose filters (Schleicher & Schnell, Inc., Dassel, Germany). The blots were pretreated in Tris-buffered saline containing 5% non-fat dry milk and 0.1% Tween 20 and then incubated with anti-iNOS antibody (Santa Cruz Biotechnology, Santa Cruz, CA, USA). Filters were washed three times and then incubated with a horseradish peroxidase-conjugated secondary antibody against goat or rabbit IgG (Amersham Pharmacia Biotech, Buckinghamshire, UK), developed using a commercial enhanced chemiluminescence system (ECL, Amersham Pharmacia Biotech, Buckinghamshire, UK). Immunoblot analysis using anti-gamma-tubulin antisera was performed as a control for protein loading. Western blot analyses of each sample were performed at least three times. Protein levels were quantified using the software Quantity One (Bio-Rad).

RNA analysis by quantitative real-time PCR

Total RNA was isolated from MKN28 cells using an RNeasy Mini kit (Qiagen) according to the manufacturer's instructions. Quantitative real-time PCR (qRT-PCR) was carried out with cDNA using the QuantiTect SYBR Green (Qiagen), gene-specific primers and an Chromo4 Real-Time thermocycler (Biorad). Gene-specific primer pairs were designed using Roche Applied Science software (<http://www.roche-applied-science.com/sis/rtPCR/upl/adc.jsp>). Primers were: Glucose-6-Phosphate Dehydrogenase, 5'-GATCTACCGCATCGACCACT-3' (G6PDF) and 5'-AGATCCTGTTGGCAAATCTCA-3' (G6PDR); iNOS, 5'-TCACGCATCAGTTTTTCAAGA-3' (iNOSF) and 5'-TCACCGTAAATATGATTTAAGTCCAC -3' (iNOSR). The reaction mixture contained 2 μ l cDNA, 0.3 μ M of primers, and 10 μ l of SYBR Green Mastermix (Qiagen), in a total volume of 20 μ l. PCR cycles were as follows: 95°C for 15 min followed by 40 cycles of 95°C for 15 s, 58°C for 30 s, and 72°C for 30 s. Each reaction was performed in triplicates. Melting curve analysis was performed to verify specificity of products. The comparative method of relative quantification (2^{-C_t}) method [35] was used to calculate expression levels of each target gene, normalized to the housekeeping gene G6PD. Data are presented as fold changes in gene expression. At least three independent experiments were performed.

Chromatin immunoprecipitation (ChIP) assays

Cross-linking was performed by adding 1% formaldehyde directly into tissue culture dishes containing 3×10^6 MKN28 at different time points after *Hp* infection, followed by incubation at room temperature for 10 min. Cells were washed twice with PBS, collected and pelleted by centrifugation at $400 \times g$ for 5 min. The pellets were resuspended in sonication buffer (containing 50 mM Tris-HCl, pH 8.1, 10 mM EDTA, 1% SDS and protease inhibitors) and incubated on ice for 10 min to lyse the nuclei. Nuclear extracts were then sonicated to obtain 400–800 bp fragments of chromatin using a 3-mm (small size) tip equipped Bandelin Sonoplus UW-2070 sonicator. Immunoprecipitation was carried out according to the protocol provided by Upstate Biotechnology (Lake Placid, NY, USA). Briefly, chromatin was diluted tenfold in ChIP dilution buffer. A small amount of chromatin was kept aside at this step to be used as input control in subsequent PCR reactions. Antibodies against acetyl-histone H3, histone H3 (dimethyl-K4) and Histone H3 (dimethyl-K9) (Abcam) were incubated with diluted chromatin at 4°C overnight. Immunoprecipitations were also carried out without Ab (no Ab controls). Protein A Sepharose (Amersham Biosciences), blocked with sheared salmon

sperm DNA, was used to collect Ab–chromatin complexes. Immune complexes were then washed once with low-salt immune complex wash buffer (containing 0.1% SDS, 1% Triton X-100, 2 mM EDTA, 20 mM Tris-HCl, pH 8.1, 150 mM NaCl), once with high-salt immune complex wash buffer (containing 0.1% SDS, 1% Triton X-100, 2 mM EDTA, 20 mM Tris-HCl, pH 8.1, 500 mM NaCl), once with LiCl immune complex wash buffer (0.25 M LiCl, 1% IGEPAL-CA630, 1% deoxycholic acid, 1 mM EDTA, 10 mM Tris-HCl, pH 8.1) and twice with sterile TE buffer. The chromatin (histone–DNA complexes) was eluted with freshly prepared elution buffer (containing 1% SDS and 0.1 M NaHCO₃), followed by reverse cross-linking with 0.3 M NaCl at 65°C for 4–5 h. DNA fragments were then purified with QIAquick spin column followed by qRT-PCR or semiquantitative PCR. Immunoprecipitated DNA recovered from ChIP assays were quantitated by qRT-PCR using a 7500 Chromo4 Real-Time thermocycler (Biorad). The primers for the iNOS promoter, used for qRT-PCR were: PNOF 5'-AAGGGGAGAGGAGGGAAAAATTGTTG-3' and PNOR, 5'-GAGGCGCTGCTGAGGAGTTCCTG-3'. The reaction mixture contained 2 μ l of ChIP or input DNA, 0.3 μ M of primers and 10 μ l of SYBR Green Mastermix (Qiagen) in a total volume of 20 μ l. PCR cycles were as follows: 95°C for 15 min followed by 40 cycles of 95°C for 15 s, 62°C for 30 s and 72°C for 30 s. Input DNA was the unbound fraction of the non-immunoprecipitated sample. Melting curve analysis revealed a single PCR product. Serial dilutions of input DNA revealed that PCR results were linear from 100 to 0.1 ng and were used to calculate absolute amounts of PCR products. No antibody controls were performed showing comparable results among the different reactions (data not shown). Results are presented as input percentage, and calculations take into account the values of at least three independent experiments.

LSD1 activity assay

Assays were performed using the colorimetric LSD1 activity assay kit (Abcam) according to the manufacturer's instructions. Briefly, 50 μ g of nuclear extracts from MKN28 cells, pretreated with 3 mM of pargyline or 2 mM TCP or with DMSO and infected with *Hp* at different times, was diluted in 49 μ l of LSD1 assay buffer, followed by addition of 1 μ l of the LSD1 substrate (H3K4me₂), and samples were incubated at 37°C for 90 min; then, 50 μ l of capture and detection antibody solution was added and incubated at room temperature for 60 and 30 min, respectively. Subsequently, the reactions were stopped by adding 100 μ l of developer solution and left for additional 10 min at room temperature away from light. Samples were then stopped and read in an ELISA plate reader at

450 nm. LSD1 activity was expressed as relative OD values per mg of protein sample. The kit provides control inhibitor and positive control assays that consist of purified LSD1 enzyme treated or not with TCP (2 mM), respectively.

Results

Induction of iNOS expression by *Hp* in MKN28 gastric cells

Hp infection of gastric mucosa leads to activation of iNOS gene [18]. In order to investigate early transcriptional events occurring at the human iNOS promoter gene upon induction by *Hp*, we utilized a human gastric epithelial cell line, MKN28, as a model. MKN28 cells were grown to confluence and incubated with bacterial suspension of *Hp* 60190 (wild-type) strain, the mutant *Hp* Tx30a or *Escherichia coli* (DH5alpha), and then iNOS mRNA levels were measured. A time-dependent increase of iNOS mRNA in response to *Hp* infection was observed (Fig. 1a). iNOS mRNA expression showed a pronounced peak at 4 h post-infection and declined after 48 h. Same experiments using a different strain of *Hp* (strain CCUG 17874) gave comparable results (data not shown) indicating that the observed pattern of iNOS induction was not related to a specific strain. Moreover, when MKN28 cells were incubated with a *VacA*-/*cagPAI*- *Hp* strain (Tx30a), a comparable increase in iNOS expression was observed (Fig. 1a) showing that iNOS activation pattern was not dependent on *VacA/CagPAI* status. Finally, to determine whether similar effects were induced by different Gram-negative bacteria, we studied the effects of *E. coli*. The infection of cells with *E. coli* DH5alpha strain did not have any effect on iNOS expression (Fig. 1a) suggesting that the observed effects were specific for *Hp*. Western blot analyses showed that levels of iNOS protein increased following a pattern consistent with that predicted by the mRNA levels (Fig. 1b, c).

Hp-induced iNOS activation is accompanied by both histone H3 acetylation and methylation modifications

In order to investigate whether specific changes in histone modifications occurred at iNOS promoter during *Hp*-induced gene activation, we performed ChIP experiments. First, we determined whether iNOS activation corresponded to increased levels of histones H3 acetylation at iNOS promoter region. Cells were incubated with *Hp* for different times, and chromatin was immunoprecipitated with anti-acetyl-H3 antibodies; then, PCR amplifications

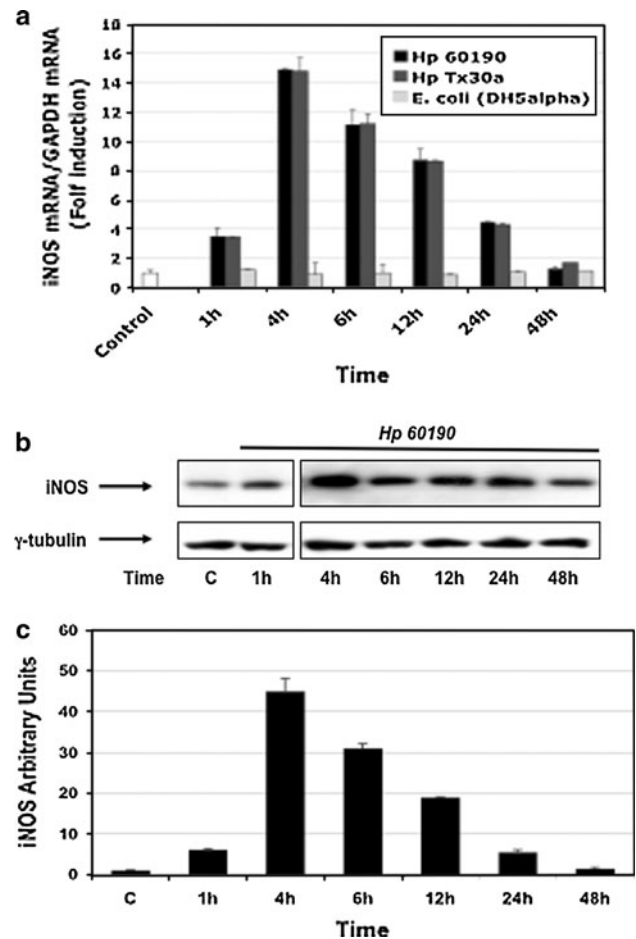


Fig. 1 *Hp* induces expression of the iNOS gene. MKN28 cells were grown to confluence and incubated with DMEM (control) or with *Hp* 60190, *Hp* Tx30a and *E. coli* (DH5alpha). **a** Total RNA was isolated at indicated time points after infection and used in qRT-PCR reactions. The iNOS levels were evaluated relative to time point 0 (control) and normalized to GAPDH levels. *Data points* represent the average of three independent experiments with the standard deviation from the mean shown. Similar results were obtained in 3 independent experiments. **b** Lysates were collected at the indicated time points after infection in RIPA buffer and 50 μ g of protein samples were loaded for electrophoresis. The expression levels of iNOS were detected using anti-iNOS antibody. The levels of tubulin were used to demonstrate equal loading. A representative blot is shown. **c** Protein levels were quantified using the software Quantity One (Bio-Rad). The iNOS protein levels were normalized to tubulin levels and expressed as relative to untreated control cells (C = control). *Data points* represent the average of three independent experiments with the standard deviation from the mean shown

were performed using promoter-specific primers (see Fig. 2a and “Materials and methods”). We found that the H3 acetylation state was transiently modulated upon infection. The histone H3, initially lowly acetylated, was highly acetylated after 4 h while the deacetylated state was restored after 48 h (Fig. 2a). Hyper-acetylation of histone H3 is in agreement with expression pattern of the iNOS

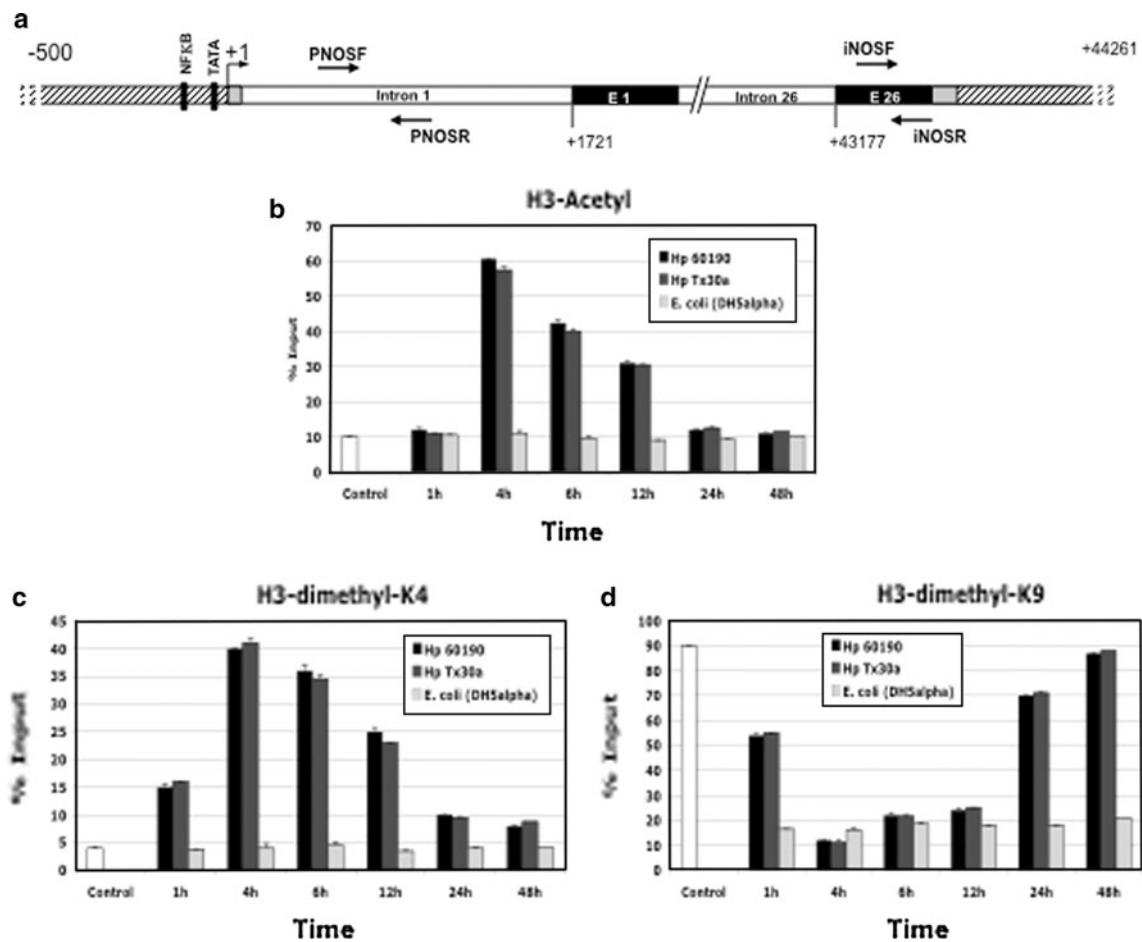


Fig. 2 *Hp*-mediated iNOS gene activation is accompanied by both histone H3 acetylation and methylation changes. **a** Schematic representation of the iNOS promoter showing the locations of PCR primers used for ChIP assay. Chromatin from MKN28 cells was harvested at the indicated time points after infection with *Hp*. Results of ChIP

analyses using anti-acetyl H3 (**b**), anti-dimethyl H3K4 (**c**) or anti-dimethyl H3K9 (**d**) antibodies are shown. Recovered DNA sequences were quantified by qRT-PCR. *Data points* represent the average of three independent experiments with the standard deviation from the mean shown

gene. Thus, H3 acetylation levels are predictive of *Hp*-mediated iNOS gene inducibility. Then, we determined whether the induction of iNOS gene upon *Hp* infection was accompanied by modification of histone methylation state at iNOS promoter. Antibodies against dimethylated H3K4 (H3K4me2) and dimethylated H3K9 (H3K9me2) were used in ChIP assays. We found that the levels of H3K4me2 were low in non-infected gastric cells and significantly increased at 4 h after *Hp* infection, returning to a near basal level by 48 h (Fig. 2c). In contrast, H3K9me2 decreased significantly in gastric epithelial cells by 1 h after *Hp* infection, with a robust decrease at 4 h, and then gradually returned to its basal state at 48 h (Fig. 2d). These results are in agreement with the repressive role of H3K9me2, with the activating role described for H3K4me2 in gene transcription [36–39] and with expression pattern of the iNOS gene.

Effect of *Hp* on the recruitment of MeCP2 at iNOS promoter

MeCP2 is known to play an important role in gene expression by recruiting H3 lysine 9 methyltransferases to promoters, thereby mediating nucleosomal H3 lysine 9 methylation [40, 41]. Since the expression of iNOS induced by *Hp*, in MKN28 cells, correlates with decreased methylation levels of histone H3K9me2, we hypothesized that *Hp* infection might mediate this effect by reducing the recruitment of MeCP2 to the iNOS promoter. To test this hypothesis, we performed ChIP assays. As shown in Fig. 3, MeCP2 was readily detected at iNOS promoter. At 4-h time point post-infection, we observed a release of MeCP2 from the iNOS promoter, and its levels were restored after 48 h (Fig. 3). These results indicated that the decreased methylation levels of H3K9me2 and the induction of iNOS

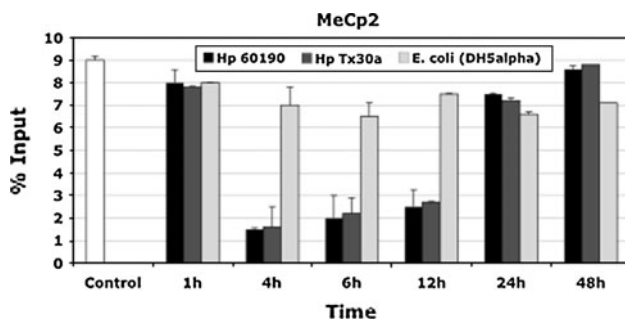


Fig. 3 Time course of *Hp*-induced binding of MeCp2 at the iNOS promoter. MKN28 cells were grown to confluence and exposed to *Hp* for the indicated time points. Chromatin was harvested and precipitated with anti-MeCp2 antibody. Recovered DNA sequences were quantified by qRT-PCR. *Data points* represent the average of three independent experiments with the standard deviation from the mean shown

transcription by *Hp* are accompanied by the release of MeCP2 from iNOS promoter.

LSD1 inhibitors reduce *Hp*-induced H3 acetylation and H3K4 methylation at the iNOS promoter and delay iNOS activation

LSD1 has both repressive (H3K4 demethylation) and activating (H3K9 demethylation) activities [42, 43]. LSD1 demethylates lysine residues via flavin–adenine dinucleotide-dependent reaction, and this reaction can be inhibited by monoamineoxidase inhibitors (MAOIs) [44–47]. Moreover, LSD1 is highly expressed in gastric adenocarcinoma [48]. For these reasons, we investigated the effect of MAOIs on *Hp*-induced H3 acetylation and H3K4 and H3K9 methylation at the iNOS promoter by chromatin immunoprecipitation (ChIP) experiments (Fig. 4). MKN28 cells were pretreated with 3 mM of pargyline or 2 mM TCP or with DMSO before infection with *Hp* at different time points. Enzymatic assays using nuclear extract of treated and untreated cells were performed as a control. These assays showed that LSD1 enzymatic activity was repressed by both pargyline and TCP (Supplemental Figure S1). ChIP analyses showed that the treatments of MKN28 cells with either pargyline or TCP led to a time-dependent decrease in levels of H3 acetylation and H3K4me2 at iNOS promoter (Fig. 4a, b). Conversely, no modifications of H3K9me2 levels were observed (Fig. 4c). Then, we investigated the impact of pargyline and TCP on *Hp*-induced iNOS activation (Fig. 5). While no significant differences in basal iNOS levels between pretreated and untreated cells were observed (time point 0), we found that iNOS activation peak was delayed from 1-h time point, observed in untreated cells, to 6-h time point when the cells were treated with either pargyline or TCP (Fig. 5).

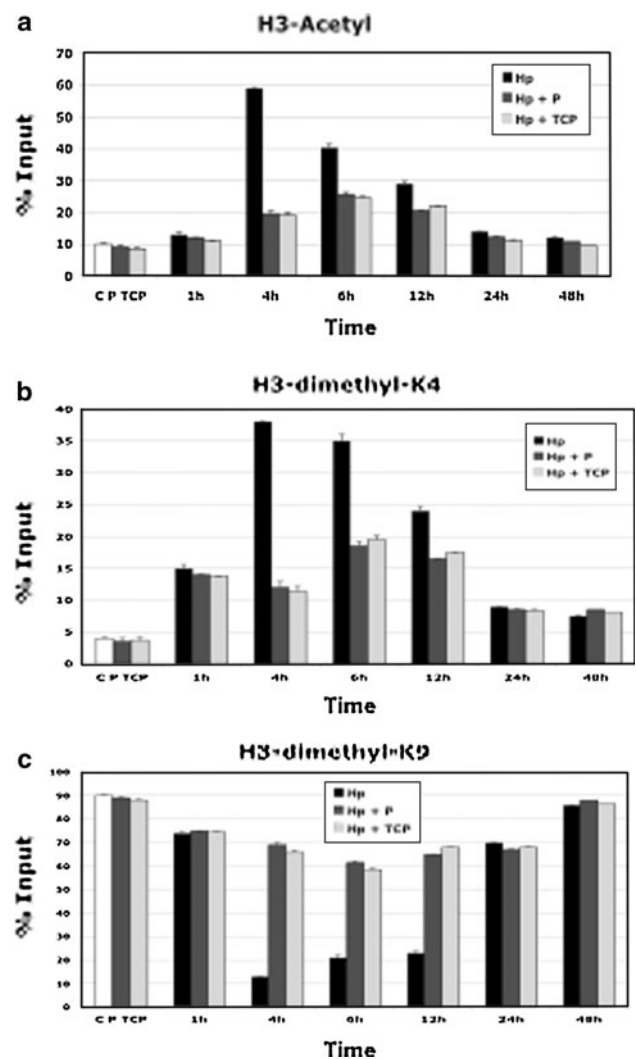


Fig. 4 Effect of pargyline and tranlycypromine on *Hp*-induced histone H3 acetylation and methylation at iNOS promoter region. MKN28 cells were grown to confluence and treated with DMSO or 3 mM pargyline (P) or 2 mM TCP (TCP) after incubation with DMEM (control) or with *Hp* 60190 for indicated time points. Results of ChIP analyses using anti-acetyl H3 (a), anti-dimethyl H3K4 (b) or anti-dimethyl H3K9 (c) antibodies are shown. Recovered DNA sequences were quantified by qRT-PCR using primers described in Fig. 4a. *Data points* represent the average of three independent experiments with the standard deviation from the mean shown

Discussion

The present study demonstrates for the first time that *Hp*-dependent iNOS activation is associated with specific chromatin modifications at the iNOS promoter. We show that (1) *Hp*-induced iNOS activation is accompanied by decreased H3K9me2 and increased H3 acetylation and H3K4me2 levels, (2) MeCP2 is released from iNOS promoter upon *Hp* infection, and (3) the activation of iNOS gene after *Hp* infection is delayed, but not eliminated, by the treatment with LSD1 inhibitors.

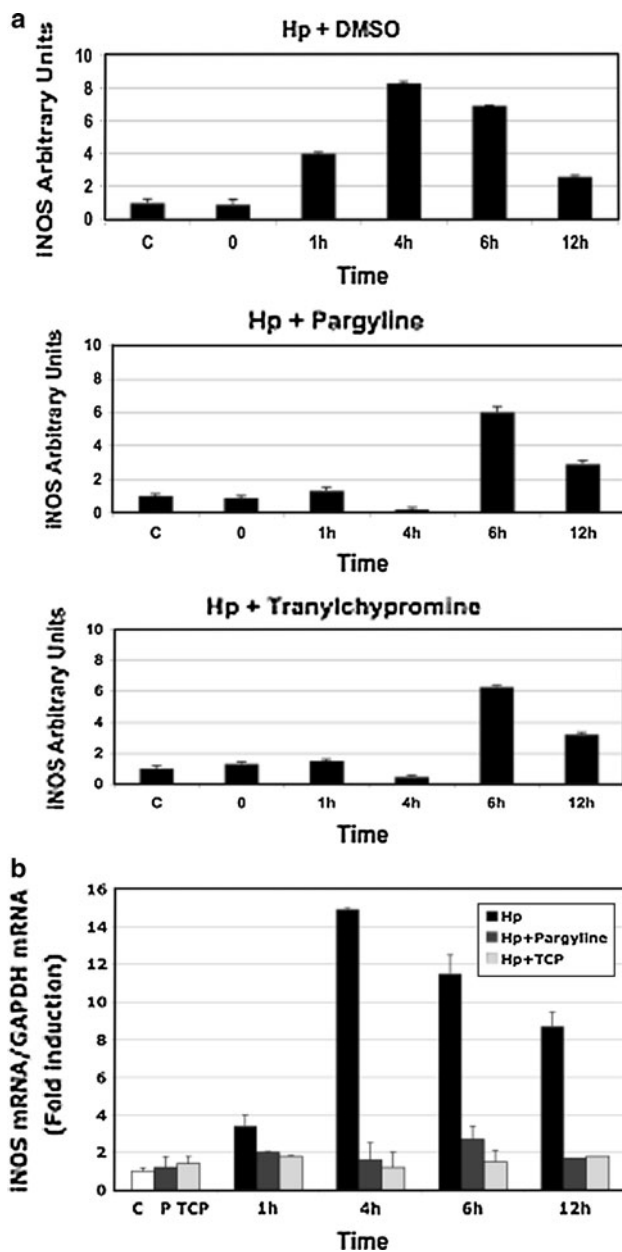


Fig. 5 LSD1 inhibitors treatment reduced *Hp*-induced iNOS gene expression. MKN28 cells were grown to confluence and treated with DMSO or 3 mM pargyline (P) or 2 mM TCP (TCP) after incubation with DMEM (control) or with *Hp* 60190 for indicated time points. **a** Protein levels were quantified using the software Quantity One (Bio-Rad). The iNOS protein levels were normalized to tubulin levels and expressed as relative to untreated control cells (C = control). iNOS protein levels before *Hp* induction and 24 h after pretreatment with DMSO, pargyline or TCP are shown (time point 0). **b** Total RNA was isolated at indicated time points after infection and used in qRT-PCR reactions. The iNOS levels were evaluated relative to control untreated cells and normalized to GAPDH levels. *Data points* represent the average of three independent experiments with the standard deviation from the mean shown

A novel strategy used by bacterial pathogens to interfere with key cellular processes may include direct effects on host epigenetics. Few recent studies demonstrate that

bacteria are indeed able to provoke histone modifications and chromatin remodelling in infected cells [49]. The effects of LPS, *Mycobacteria*, *Shigella*, *Listeria* and *Helicobacter* on some aspects of host epigenetics have been recently reported [49]. It has been shown that the expression of IL-6 is modulated by *Hp* through activation of ERK/p38/MSK1 cascade and consequent H3S10 phosphorylation, which in turn is necessary for IL-6 activation [26]. We have recently demonstrated that chromatin and DNA methylation modifications accompany *Hp*-induced Cox-2 activation in gastric epithelial cells [27]. Another important aspect linking epigenetic modification to *Hp* infection are the well established alterations of chromatin and DNA methylation profiles described at several loci in gastrointestinal cancers [50–52]. However, conflicting data are reported about the direct involvement of pre-existing *Hp* infection of gastric mucosa as a determining factor for epigenetic alterations observed in gastric diseases. We should consider that many events, including inflammation, cancer progression and stochastic epigenetic changes, may occur between *Hp* infection and clinical diagnosis, and thus it is expected that a wide spectrum of epigenetic alterations may be observed in pathologic samples regardless of those directly provoked by the *Hp* infection.

In this work, we have investigated the epigenetic changes occurring at iNOS locus during the first 48 h after exposure of gastric cells to *Hp* and, thus, directly attributable to host–parasite interaction. We show that MKN28 cells express iNOS mRNA and proteins weakly under the unstimulated condition, and the expression levels increase dramatically upon *Hp* stimulation concomitantly with the occurrence of several chromatin changes. A role of histone acetylation in the regulation iNOS gene was previously suggested in studies performed in macrophages cells under different kind of stimulation [53]. In this work, we have shown that transient changes of the histone H3 acetylation state accompany the first phases of *Hp* infection of gastric cells. Modulation of histone deacetylase expression in *Hp*-exposed gastric cells has been recently described in an animal model [54]. Moreover, our results indicate that the main drivers of iNOS activation upon *Hp* exposure are the increase in H3K4me2 levels and the decrease in H3K9 methylation state. Accordingly, previous reports indicate that the increase in H3K4me2, as well as the decrease in H3K9me2 levels, marks transcriptionally active chromatin structure [36–39].

Because LSD1 has both repressive and activating effects through H3K4 and H3K9 demethylation capability [42, 43], we investigated *Hp*-dependent histone modification occurring in MKN28 cells pretreated with LSD1 inhibitors. We show that both pargyline and TCP have no effects on iNOS basal levels while both inhibitors have a strong influence on *Hp*-induced iNOS activation. In fact,

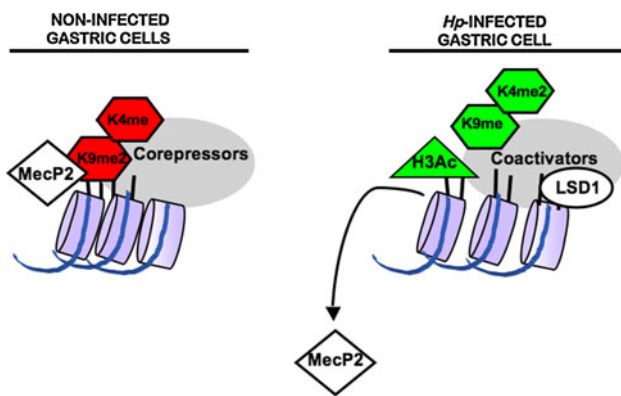


Fig. 6 A schematic model illustrating a possible sequence of epigenetic events at iNOS gene during *Hp*-induced activation. MeCP2 methyl-CpG-binding protein 2, LSD1 Lysine-specific demethylase 1

both LSD1 inhibitors repress *Hp*-dependent iNOS activation during the first 4 h after *Hp* infection; however, they cannot prevent the iNOS induction at later times (6 h). This phenomenon could be explained by the fact that early *Hp*-dependent iNOS activation requires LSD1 (or other monoamineoxidase) activity while the later iNOS peak (6 h) may be the result of different putative enzymatic activity. Our data suggest a model in which LSD1, limited to the first phases of infection, and MeCP2 may play an intermediary role between repressive and active histone marks by removing methylation and providing the naked lysine residue to be acetylated (Fig. 6).

Further studies will possibly elucidate the wide variety of epigenetic profiles observed at iNOS gene in gastritis and gastric tumours that may be a result of different mechanisms including those derived by direct host–parasite interaction and additional events occurring during inflammation and cancer progression.

Acknowledgments This work was supported by grant from MIUR and from Regione Campania to LC.

Conflict of interest There were no conflicts of interest with any of the authors.

References

1. Parsonnet J, Vandersteen D, Goates J, Sibley RK, Pritikin J, Chang Y (1991) *Helicobacter pylori* infection in intestinal- and diffuse-type gastric adenocarcinomas. *J Natl Cancer Inst* 9:640–643
2. Erkisi M, Colakoglu S, Köksal F, Tuncer I, Burgut R, Karaköse H, Doran F, Zorludemir S (1997) Relationship of *Helicobacter pylori* infection to several malignant and non-malignant gastrointestinal diseases. *J Exp Clin Cancer Res* 3:289–293

3. Komoto K, Haruma K, Kamada T, Tanaka S, Yoshihara M, Sumii K, Kajiyama G, Talley NJ (1998) *Helicobacter pylori* infection and gastric neoplasia: correlations with histological gastritis and tumor histology. *Am J Gastroenterol* 93:1271–1276
4. Wang CC, Wu MS, Wang HH, Wang HP, Lee WC, Shun CT, Lin JT (1998) *Helicobacter pylori* infection and age on the development of intestinal metaplasia—a multiple logistic regression analysis. *Hepatogastroenterology* 45:2234–2237
5. You WC, Zhang L, Gail MH, Chang YS, Liu WD, Ma JL, Li JY, Jin ML, Hu YR, Yang CS, Blaser MJ, Correa P, Blot WJ, Fraumeni JF Jr, Xu GW (2000) Gastric dysplasia and gastric cancer: *Helicobacter pylori*, serum vitamin C, and other risk factors. *J Natl Cancer Inst* 19:1607–1612
6. Peek RM, Blaser MJ (2002) *Helicobacter pylori* and gastrointestinal tract adenocarcinomas. *Nat Rev Cancer* 2:28–37
7. Watanabe T, Tada M, Nagai H, Sasaki S, Nakao M (1998) *Helicobacter pylori* infection induces gastric cancer in mongolian gerbils. *Gastroenterology* 115:642–648
8. Zheng Q, Chen XY, Shi Y, Xiao SD (2004) Development of gastric adenocarcinoma in Mongolian gerbils after long-term infection with *Helicobacter pylori*. *J Gastroenterol Hepatol* 19:1192–1198
9. Gerhard M, Lehn N, Neumayer N, Borén T, Rad R, Schopp W, Miehke S, Classen M, Prinz C (1999) Clinical relevance of the *Helicobacter pylori* gene for blood-group antigen-binding adhesin. *Proc Natl Acad Sci USA* 96:12778–12783
10. van Doorn LJ, Figueiredo C, Sanna R, Plaisier A, Schneeberger P, de Boer W, Quint W (1998) Clinical relevance of the cagA, vacA, and iceA status of *Helicobacter pylori*. *Gastroenterology* 115:58–66
11. Franco AT, Johnston E, Krishna U, Yamaoka Y, Israel DA, Nagy TA, Wroblewski LE, Piazuelo MB, Correa P, Peek RM Jr (2008) Regulation of gastric carcinogenesis by *Helicobacter pylori* virulence factors. *Cancer Res* 2:379–387
12. Uno K, Kato K, Atsumi T, Suzuki T, Yoshitake J, Morita H, Ohara S, Kotake Y, Shimosegawa T, Yoshimura T (2007) Toll-like receptor (TLR) 2 induced through TLR4 signaling initiated by *Helicobacter pylori* cooperatively amplifies iNOS induction in gastric epithelial cells. *Am J Physiol Gastrointest Liver Physiol* 5:1004–1012
13. Chang YJ, Wu MS, Lin JT, Sheu BS, Muta T, Inoue H, Chen CC (2004) Induction of cyclooxygenase-2 overexpression in human gastric epithelial cells by *Helicobacter pylori* involves TLR2/TLR9 and c-Src-dependent nuclear factor-kappaB activation. *Mol Pharmacol* 66:1465–1477
14. Kim JM, Kim JS, Jung HC, Oh YK, Chung HY, Lee CH, Song IS (2003) *Helicobacter pylori* infection activates NF-kappaB signaling pathway to induce iNOS and protect human gastric epithelial cells from apoptosis. *Am J Physiol Gastrointest Liver Physiol* 6:1171–1180
15. Lim JW, Kim H, Kim KH (2001) NF-kappaB, inducible nitric oxide synthase and apoptosis by *Helicobacter pylori* infection. *Free Radic Biol Med* 3:355–366
16. Naito Y, Yoshikawa T (2005) Carcinogenesis and chemoprevention in gastric cancer associated with *Helicobacter pylori* infection. Role of oxidants and antioxidants. *J Clin Biochem Nutr* 236:37–49
17. Naito Y, Yoshikawa T (2002) Molecular and cellular mechanisms involved in *Helicobacter pylori*-induced inflammation and oxidative stress. *Free Radic Biol Med* 33:323–336
18. Fu S, Ramanujam KS, Wong A, Fantry GT, Drachenberg CB, James SP, Meltzer SJ, Wilson KT (1999) Increased expression and cellular localization of inducible nitric oxide synthase and cyclooxygenase 2 in *Helicobacter pylori* gastritis. *Gastroenterology* 116:1319–1329

19. Liu RH, Hotchkiss JH (1995) Potential genotoxicity of chronically elevated nitric oxide: a review. *Mutat Res* 339:73–89
20. Fukumura D, Jain RK (1998) Role of nitric oxide in angiogenesis and microcirculation in tumors. *Cancer Metastasis Rev* 17:77–89
21. Kolb H, Kolb BV (1992) Nitric oxide: a pathogenetic factor in autoimmunity. *Immunol Today* 13:157–160
22. Kim SF, Huri DA, Snyder SH (2005) Inducible nitric oxide synthase binds, S-nitrosylates, and activates cyclooxygenase-2. *Science* 310:1966–1970
23. Lejeune P, Lagadec P, Onier N, Pinar D, Ohshima H, Jeannin JF (1994) Nitric oxide involvement in tumor-induced immunosuppression. *J Immunol* 10:5077–5083
24. Suzuki H, Hibi T, Marshall BJ (2007) *Helicobacter pylori*: present status and future prospects in Japan. *J Gastroenterol* 42:1–15
25. Chan C, Li L, McCall CE, Yoza BK (2005) Endotoxin tolerance disrupts chromatin remodeling and NF-kappaB transactivation at the IL-1beta promoter. *J Immunol* 1:461–468
26. Pathak SK, Basu S, Bhattacharyya A, Pathak S, Banerjee A, Basu J, Kundu M (2006) TLR4-dependent NF-kappaB activation and mitogen- and stress-activated protein kinase 1-triggered phosphorylation events are central to *Helicobacter pylori* peptidyl prolyl cis-, trans-isomerase (HP0175)-mediated induction of IL-6 release from macrophages. *J Immunol* 11:7950–7958
27. Pero R, Peluso S, Angrisano T, Tuccillo C, Sacchetti S, Keller S, Tomaiuolo R, Bruni CB, Lembo F, Chiariotti L (2011) Chromatin and DNA methylation dynamics of *Helicobacter pylori*-induced COX-2 activation. *Int J Med Microbiol* 2:140–149
28. Angrisano T, Pero R, Peluso S, Keller S, Sacchetti S, Bruni CB, Chiariotti L, Lembo F (2010) LPS-induced IL-8 activation in human intestinal epithelial cells is accompanied by specific histone H3 acetylation and methylation changes. *BMC Microbiol* 14:10–172
29. Motoyama T, Hojo H, Watanabe H (1986) Comparison of seven cell lines derived from human gastric carcinomas. *Acta Pathol* 36:65–83
30. Romano M, Ricci V, Memoli A, Tuccillo C, Di Popolo A, Sommi P, Acquaviva AM, Del Vecchio BC, Bruni BC, Zarrilli R (1998) *Helicobacter pylori* up-regulates cyclooxygenase-2 mRNA expression and prostaglandin E₂ synthesis in MKN 28 gastric mucosal cells in vitro. *J Biol Chem* 273:28560–28563
31. Le'Negrate G, Ricci V, Hofman V, Mograbi B, Hofman P, Rossi B (2001) Epithelial intestinal cell apoptosis induced by *Helicobacter pylori* depends on expression of the cag pathogenicity island phenotype. *Infect Immun* 8:5001–5009
32. Atherton JC, Cao P, Peek RM Jr, Tummuru MK, Blaser MJ, Cover TL (1995) Mosaicism in vacuolating cytotoxin alleles of *Helicobacter pylori*. Association of specific vacA types with cytotoxin production and peptic ulceration. *J Biol Chem* 30:17771–17777
33. Aras RA, Lee Y, Kim SK, Israel D, Peek RMJ, Blaser MJ (2003) Natural variation in populations of persistently colonizing bacteria affect human host cell phenotype. *J Infect Dis* 4:4486–4496
34. Cover TL, Dooley CP, Blaser MJ (1990) Characterization of and human serologic response to proteins in *Helicobacter pylori* broth culture supernatants with vacuolizing cytotoxin activity. *Infect Immun* 58:603–610
35. Livak KJ, Schmittgen TD (2001) Analysis of relative gene expression data using real-time quantitative PCR and the 2(-Delta Delta C(T)) method. *Methods* 25:402–408
36. Kouzarides T (2007) Chromatin modifications and their function. *Cell* 128:693–705
37. Jenuwein T, Allis CD (2001) Translating the histone code. *Science* 293:1074–1080
38. Turner BM (2007) Defining an epigenetic code. *Nat Cell Biol* 9:2–6
39. Berger SL (2007) The complex language of chromatin regulation during transcription. *Nature* 447:407–412
40. Georgel PT, Horowitz-Scherer RA, Adkins N, Woodcock CL, Wade PA, Hansen JC (2003) Chromatin compaction by human MeCP2. Assembly of novel secondary chromatin structures in the absence of DNA methylation. *J Biol Chem* 34:32181–32188
41. Fuks F, Hurd PJ, Wolf D, Nan X, Bird AP, Kouzarides T (2003) The methyl-CpG-binding protein MeCP2 links DNA methylation to histone methylation. *J Biol Chem* 6:4035–4040
42. Lee MG, Wynder C, Cooch N, Shiekhatter R (2005) An essential role for CoREST in nucleosomal histone 3 lysine 4 demethylation. *Nature* 437:432–435
43. Shi YJ, Matson C, Lan F, Iwase S, Baba T, Shi Y (2005) Regulation of LSD1 histone demethylase activity by its associated factors. *Mol Cell* 6:857–864
44. Metzger E, Wissmann M, Yin N, Müller JM, Schneider R, Peters AH, Günther T, Buettner R, Schüle R (2005) LSD1 demethylates repressive histone marks to promote androgen-receptor-dependent transcription. *Nature* 437:436–439
45. Lee MG, Wynder C, Schmidt DM, McCafferty DG, Shiekhatter R (2006) Histone H3 lysine 4 demethylation is a target of non-selective antidepressive medications. *Chem Biol* 6:563–567
46. Schmidt DM, McCafferty DG (2007) trans-2-Phenylcyclopropylamine is a mechanism-based inactivator of the histone demethylase LSD1. *Biochemistry* 46:4408–4416
47. Yang M, Culhane JC, Szewczuk LM, Jalili P, Ball HL, Machius M, Cole PA, Yu H (2007) Structural basis for the inhibition of the LSD1 histone demethylase by the antidepressant trans-2-phenylcyclopropylamine. *Biochemistry* 46:8058–8065
48. Magerl C, Ellinger J, Braunschweig T, Kremmer E, Koch LK, Höller T, Büttner R, Lüscher B, Gütgemann I (2010) H3K4 dimethylation in hepatocellular carcinoma is rare compared with other hepatobiliary and gastrointestinal carcinomas and correlates with expression of the methylase Ash2 and the demethylase LSD1. *Hum Pathol* 2:181–189
49. Hamon MA, Cossart P (2008) Histone modifications and chromatin remodeling during bacterial infections. *Cell Host Microbe* 2:100–109
50. de Maat MF, van de Velde CJ, Umetani N, de Heer P, Putter H, van Hoesel AQ, Meijer GA, van Grieken NC, Kuppen PJ, Bilchik AJ, Tollenaar RA, Hoon DS (2007) Epigenetic silencing of cyclooxygenase-2 affects clinical outcome in gastric cancer. *J Clin Oncol* 31:4887–4894
51. Perri F, Cotugno R, Piepoli A, Merla A, Quitadamo M, Gentile A, Pilotto A, Annese V, Andriulli A (2007) Aberrant DNA methylation in non-neoplastic gastric mucosa of *H. pylori* infected patients and effect of eradication. *Am J Gastroenterol* 7:1361–1371
52. Maekita T, Nakazawa K, Mihara M, Nakajima T, Yanaoka K, Iguchi M, Arii K, Kaneda A, Tsukamoto T, Tatematsu M, Tamura G, Saito D, Sugimura T, Ichinose M, Ushijima T (2006) High levels of aberrant DNA methylation in *Helicobacter pylori*-infected gastric mucosae and its possible association with gastric cancer risk. *Clin Cancer Res* 12:989–995
53. Deng WG, Wu KK (2003) Regulation of inducible nitric oxide synthase expression by p300 and p50 acetylation. *J Immunol* 2:6581–6588
54. Saito Y, Suzuki H, Tsugawa H, Suzuki S, Matsuzaki J, Hirata K, Hibi T (2011) Dysfunctional gastric emptying with down-regulation of muscle-specific microRNAs in *Helicobacter pylori*-infected mice. *Gastroenterology* 140:189–198